

# Teleoperation Controller Design using $H_\infty$ -Optimization with Application to Motion-Scaling

Joseph Yan and S.E. Salcudean

*Abstract*—The design of a bilateral teleoperation controller is a nontrivial problem. The goal is to achieve a stable system with optimal performance in the possible presence of time delays, disturbances, uncertainties and/or measurement noise. In this paper, a general design strategy based on  $H_\infty$  theory is presented. This approach allows a convenient means to tradeoff the optimization of various performance criteria and system robustness. The control approach is applied to a motion-scaling teleoperation system and simulations and experiments with the resulting controllers demonstrate that the strategy is effective.

## I. INTRODUCTION

Teleoperation may be viewed as that branch of robotics which concerns the manipulation of environments or spaces generally inaccessible to man. The basic teleoperation system consists of a *slave* device tracking a *master* device directly manipulated by a human operator as in Figure 1. When the master is also actuated based on sensor signals from the slave, such a system is described as being *bilateral*. The kinesthetic sensations provided in bilateral teleoperators can substantially enhance operator performance both in speed and safety [1], [2].

### Motion-Scaling Application

The usual applications cited for teleoperation are in space exploration, nuclear waste handling and subsea exploration where the environments are hazardous and it is preferable to have the operator remotely located at a safer and more comfortable site. Another domain which is increasingly being exploited is magnitude scaling of forces and motions. At the microscopic level, this concept is used to improve resolution as demonstrated by systems which allow the manipulation of individual biological cells [3] or give the perception of feeling atomic surfaces [4]. At the other end of the spectrum, human capacity can be increased, for example, through the use of man-amplifiers or exoskeletal extenders which magnify the operator's strength and motions [5].

The work presented in this paper was motivated by a project at the University of British Columbia (UBC) involving the development of a prototype telerobotic system for use in microsurgery experiments [6], [7]. The system

Joseph Yan was a M.A.Sc. student in the Department of Electrical Engineering at the University of British Columbia. He is now with QUADRALOGIC Technologies Inc. of Vancouver, B.C.

S.E. Salcudean is with the Department of Electrical Engineering at the University of British Columbia.

This work was supported by the Science Council of British Columbia, the IRIS Network of Centres of Excellence and an NSERC Scholarship.

scales down movements from the operator's hand to the slave tool while, simultaneously, magnifying forces exerted on the tool to the hand. Such a system would be extremely useful in facilitating microsurgery by significantly increasing a surgeon's level of dexterity.

The motion-scaling system, illustrated in Figure 2, consists of two fine-motion magnetically-levitated, or *maglev*, wrists [8], [9] (a *macro-master* and a *micro-slave*). Each fine-motion maglev wrist consists of two rigid elements – a magnetic-field-generating *stator* and a lightweight, rigid *flotor* with conducting coils located in the magnetic gaps. Levitation of the flotor arises from Lorentz forces generated between the two elements when current is passed through the coils. The maglev wrists were chosen for their superior positioning and force application capabilities in a 6 degree-of-freedom (DOF) workspace.

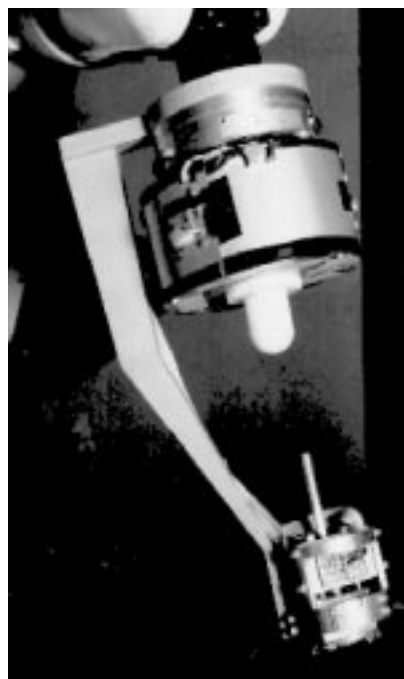


Fig. 2. Dual Wrist Assembly

This dual wrist assembly is used as the design example for the controller presented in this paper. More detailed information of the system can be found in [6], [7].

### Controller Design

In general, the performance of a teleoperator depends on the quality of both the actuation mechanisms and the controller employed. In this paper, design for the second item

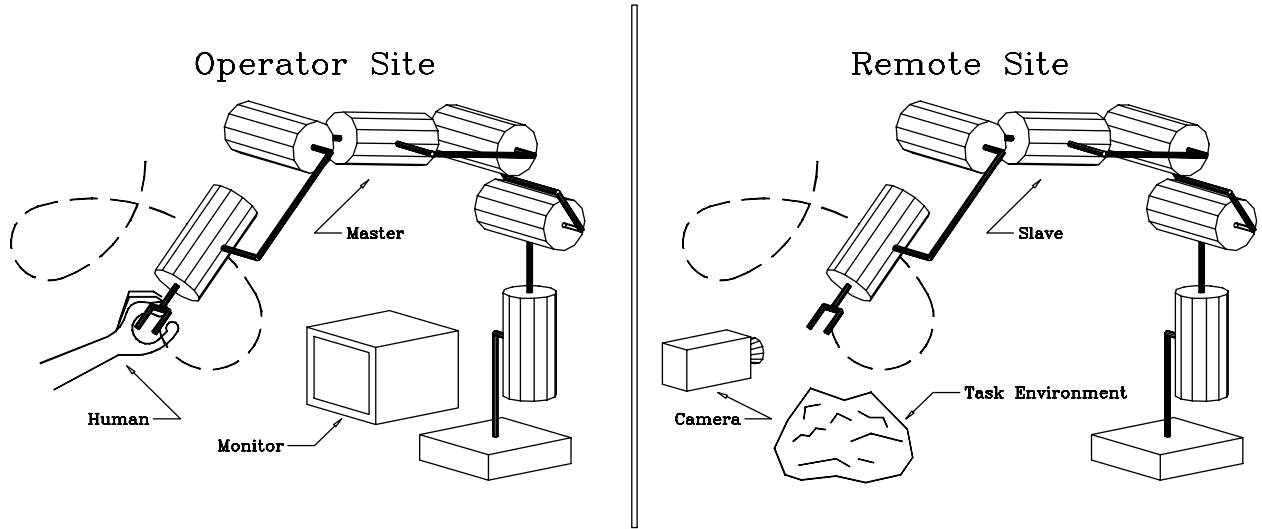


Fig. 1. Basic Teleoperation

is addressed although knowledge of the actuator characteristics and limitations are useful for the model.

A telemanipulator with a poorly-designed controller will provide inferior performance regardless of the quality of actuation. In general, the goal in the bilateral controller design problem is to realize a stable system with “optimal” performance. The problem is a difficult one because the desired dynamics largely depend on the application. For example, in some situations, position control is more important than force control but in other situations, the reverse is true. Furthermore, these can be viewed as the two extremes of the impedance control spectrum. The presence of time delays, disturbances, uncertainties and/or measurement noise have the effect of destabilizing the system and these problems must be addressed in the controller design. There is a basic tradeoff between improving the controller performance and in increasing the system robustness.

Development of a reasonably accurate model of the system is important to the synthesis and analysis of controllers. A commonly used model is one with five separate subsystems as shown in Figure 3, *e.g.*, [10], [11], [12]. The master, controller, and slave can be grouped into a single block representing the teleoperator as shown by the dashed line, *e.g.*, [13], [14], [15]. The operator and task environment each interact with a single subsystem (*i.e.*, their respective manipulators). The master and slave manipulators each interact with their respective environments (the operator can be considered to be the “master’s environment”) and the controller. The arrows indicate that the information flow can be in either direction. However, a signal “entering” the controller is a measured quantity whereas one “exiting” is a desired setpoint. The operator and environment should be included in the model because when they interact with the teleoperator, the system dynamics may be significantly altered. For simplicity, the blocks are usually modeled as linear, time-invariant (LTI) systems in which the dynamics of the force transmission and position responses can be mathematically character-

ized by a set of network functions. This allows the designer to draw upon well-developed network theory for synthesis and analysis of the controller.

Two useful concepts from network theory are *passivity* and *scattering matrices*. Physically, a device is passive if it cannot increase the total energy of a system in which it is an element (assuming it has no initial energy); hence, passive systems are inherently stable. Mathematically, an  $n$ -port is passive *iff* for any set of injected flows ( $v$ ) and applied efforts ( $f$ ) satisfying its network function, the inequality

$$\int_0^{\infty} f^T(t)v(t)dt \geq 0 \quad (1)$$

is satisfied. The scattering matrix of a system is the mathematical network function  $S(s)$  mapping efforts plus flows into efforts minus flows [16], *i.e.*, satisfying the equation

$$f(s) - v(s) = S(s)[f(s) + v(s)] \quad (2)$$

It can be shown that a system is passive *iff* the  $\infty$ -norm of its scattering matrix is no greater than unity (*i.e.*,  $\|S\|_{\infty} \leq 1$ ) [16]. It may even be loosely argued that systems with smaller scattering matrix norms have greater stability margins.

Colgate and Hogan showed that when a network is coupled to a passive environment, then passivity of the network interaction port is sufficient for stability and is also necessary when dealing with *any* passive environment [17]. Thus, a model often used is a 2-port teleoperator in contact with a passive 1-port environment; in this case, the designer only needs to ensure passivity of the teleoperator to guarantee stability (*e.g.*, [13], [14], [10]). More recently, it has been shown that knowledge of the teleoperator structure allows a less conservative design [18], [19]; the necessary and sufficient requirement for coupled stability to a passive environment and passive operator is that the structured singular value  $\mu(S)$  of the teleoperator scattering matrix be no greater than unity, or

$$\mu(S) = [\inf(\bar{\sigma}(\Delta)|\det(I - S\Delta) = 0)]^{-1} \quad (3)$$

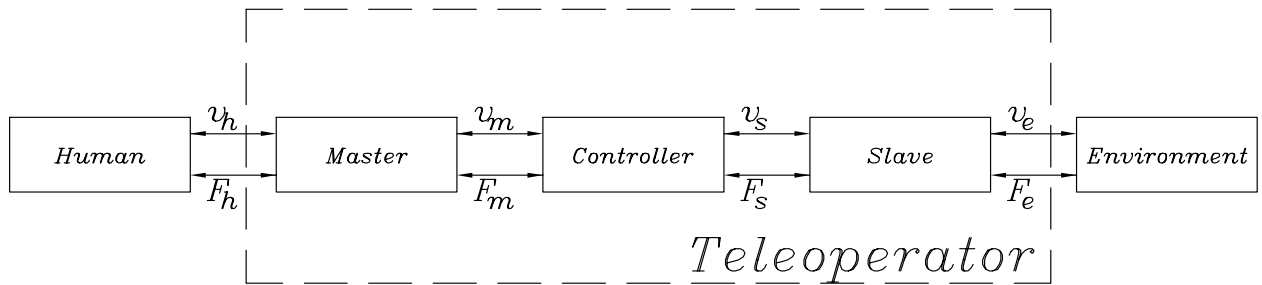


Fig. 3. General Teleoperation Model

Note that if the limited range of environment impedances encountered is known, then either of the above requirements may be considered overly conservative; alternatively, if the environment possesses an active state-dependent term, then there is no guarantee of absolute stability.

Hogan proposed impedance control as a strategy to control the amount of mechanical work exchanged at the manipulator/environment interface by modulating the dynamic behavior of the manipulator [20]. Although teleoperation is not specifically discussed by Hogan, it is an area in which the impedance controller described can be used. Indeed, impedance controllers for telemanipulators are described in a number of papers. Hannaford proposed bilateral impedance control employing estimators to identify the operator and environment impedances which are then used to modulate the manipulator impedances [21]. In [18], Colgate provides an insightful discussion on designing a bilateral manipulator to “shape” the perceived environment impedance, with special attention given to systems in which the dynamics of the master and slave are not desired to be the same; use of the structured singular value  $\mu$  to provide robust impedance shaping is also discussed. An impedance controller is used with impedance matching in [11] by Niemeyer and Slotine for preventing reflections in a passive controller. The success of impedance control depends on the availability and accuracy of the environment model and perhaps this is the most significant drawback.

Time delays have a destabilizing effect on bilateral teleoperators and this problem is addressed by Anderson and Spong [10]. It is shown that delays in the communication block make the standard control law non-passive but by mimicking a lossless transmission line, the system becomes passive and, hence, stable. Niemeyer and Slotine provide an extension to this passivity-based approach by looking at the application of impedance control and using an energy-based derivation in which wave variables representing power are transmitted [11]. By using a symmetric configuration with an impedance controller on either side of the communication block, impedances can be matched at both sides to prevent wave reflections which corrupt the flow of useful information. Lawn and Hannaford experimentally test the passivity concept of [10] and conclude that the stability guarantee comes at the expense of reduced stiffness, resulting in poor teleoperator transparency [22].

Leung *et al.* also treat the time delay problem but use

a combined  $H_\infty$ -optimization and  $\mu$ -synthesis framework to design a teleoperator which is stable for a pre-specified time delay while optimizing performance characteristics [12]. The first stage of the design considers the slave to be in free motion so an operator force results in motion of the master and corresponding motion of the slave without any slave dynamics being fed back to the master; the second stage assumes constrained motion so that a measured environment contact force results in master actuation forces to reflect this interaction.

The use of  $H_\infty$  theory in bilateral controller design is also proposed by Salcudean *et al.* in [23]. The suggested control law feeds measured hand and environment forces to the slave and master actuators, respectively, along with a “coordinating force” based on the positional error. A parameterization of all coordinating force transfer functions which stabilize the system can then be obtained.  $H_\infty$ -optimization is used to find the parameter which best shapes the closed-loop response (minimize the tracking error and maximize transparency).

Kazerooni *et al.* applied  $H_\infty$  control theory to shape the relationships between forces and positions at both ends of the teleoperator [24]. The approach was to minimize a weighted error between the actual and desired transfer functions for positions and forces using a “force-force” architecture. The control signals are based only on the measured contact forces which could, possibly, result in a positional error between the master and slave manipulators. Relative to the contribution of [24], this paper presents a “four-channel” architecture, proposed in [15], [14], [23], in which the control signals are based on positions as well as on forces, and considers noise disturbances and weighting functions that can be used to trade off teleoperator performance *vs* stability robustness. The ability to perform such tradeoffs is demonstrated with simulations and experiments with a motion-scaling system.

### Ideal Teleoperation Control

Teleoperator performance might be quantified by how closely it behaves like the “ideal teleoperator”. One viewpoint of this arises from a human factors standpoint. Here, the dynamics of each manipulator would be adjusted to fit the operator preferences and the application [13], [25], [18]. The dynamics might even be continuously varied to reduce fatigue and improve precision. Although this view of an impedance shaping and/or time-varying teleoperation has merit, it will not be used here because of the high depen-

dence on the human subject and on the task at hand.

Instead, the more conventional definition will be adopted in which the ideal teleoperator is one which provides complete *transparency* of the man-machine interface (*i.e.*, the operator has the perception of working directly on the task environment). In [14], this is suggested to be the case if the position and force responses of the master and slave arms are absolutely equal, respectively, when an operating force is applied to the system. Lawrence describes perfect transparency as the case in which the impedance transmitted to the master is identical to the task environment impedance [15]. Although these descriptions assume one-to-one correspondence between the master and slave, they can readily be adapted for the case of magnitude scaling teleoperators. In such a case it is reasonable to describe ideal teleoperation as having the position and force responses of the master being scaled constant multiples of the slave respective responses and so the impedance transmitted is also a constant multiple of the environment impedance.

To demonstrate this concept, consider the previously described maglev motion-scaling teleoperation system [6], [7]. The master and slave flotors can be modeled as rigid bodies in free space. The single DOF case is depicted in Figure 4. The bodies obey the following equations of motion (Laplace transforms are assumed throughout):

$$\begin{aligned} m_m s^2 x_m &= f_h + f_{ma} = f_{ha} - H x_m + f_{ma} \\ m_s s^2 x_s &= f_e + f_{sa} = f_{ea} - E x_s + f_{sa} \end{aligned} \quad (4)$$

where  $m_m, m_s, x_m, x_s, f_{ma}$ , and  $f_{sa}$  are, respectively, the master and slave masses, positions and actuator forces. The operator hand force  $f_h$  and environment force  $f_e$  are each considered to possess active exogenous components  $f_{ha}$  and  $f_{ea}$ , respectively, and passive feedback components  $f_{hp} = -H x_m$  and  $f_{ep} = -E x_s$  where  $H$  and  $E$  represent the hand and environment “impedances”, respectively. In this paper, the impedance represents the mapping from position to force (as in [15]) instead of the conventionally used transfer function mapping velocity to force (as in [13]). This is because it is notationally more convenient to use a single function to relate signals of interest which, in most cases, are position and force. When the task is simply manipulation of an object of mass  $m$  in free space, the dynamics of the object satisfy Newton’s second law of motion,  $F = m s^2 x$ , where  $F$  is the externally applied force and  $x$  is the mass position;  $E$  would be represented by  $m s^2$ . If the manipulator is moving through a fluid with damping  $b$ ,  $E$  would more accurately be described by  $bs$ . When contacting an object obeying Hooke’s Law with stiffness  $k$ ,  $E$  would simply be  $k$  (assuming the mass is negligible). Most tasks can be reasonably modeled as a linear combination of these three in the familiar mass-spring-damper system in which the impedance is  $m s^2 + b s + k$ . Although assumed to be linear in this paper, often  $H$  and  $E$  are non-linear operators (*e.g.*, when the slave is in contact with a stiff environment). Linear models for the hand have been motivated and obtained in [24]. Nonlinear models for the hand and environment dynamics and a discussion of stability issues for contact tasks can be found in [26].

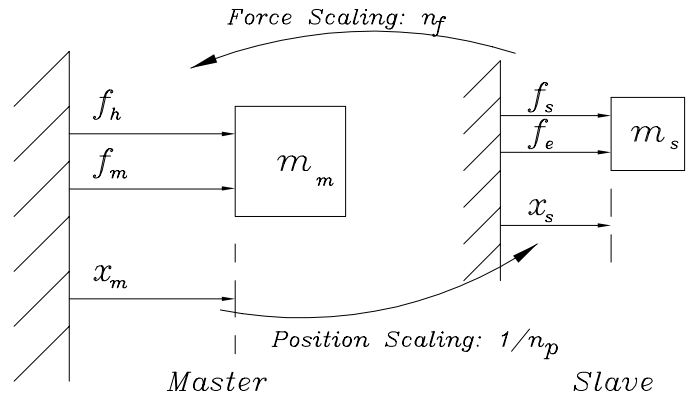


Fig. 4. 1-DOF Teleoperation

For identical master/slave systems and unity scaling ratios, ideal teleoperation can be realized by setting  $f_{ma} = f_e$  and  $f_{sa} = f_h$ , where hand and environment force measurements are assumed to be available and exact. A small position error term (coordinating force) can be added to insure that errors in initial conditions converge to zero. For a bilateral motion-scaling and force-scaling system, consider that the upward force-scaling ratio  $n_f$  and the downward motion-scaling ratio  $n_p$  are independently chosen constants (*i.e.*, the goals are  $f_{ma} = n_f f_e$  and  $x_m = n_p x_s$ ). Then, for a mass ratio  $n_m = m_m/m_s$ , these desired scalings are achieved with the control law

$$\begin{aligned} f_{ma} &= n_f f_e \\ f_{sa} &= \frac{f_h + (n_f - n_m n_p) f_e}{n_m n_p} \end{aligned} \quad (5)$$

This results in the following equations relating exogenous forces to positions:

$$\begin{aligned} f_{ha} + n_f f_{ea} &= \left( m_m s^2 + H + \frac{n_f E}{n_p} \right) x_m \\ \frac{f_{ha}}{n_f} + f_{ea} &= \left( \frac{n_p n_m}{n_f} m_s s^2 + \frac{n_p H + E}{n_f} \right) x_s \end{aligned} \quad (6)$$

Equation (5) shows that when  $n_f = n_m n_p$ , the force-scaling from master to slave is  $1/n_f$ , as one might expect. However, when  $n_f \neq n_m n_p$ , there is a local feedback term at the slave making its “apparent” mass a scaling of the actual mass by  $n_p n_m/n_f$ , as seen in (6). At the master end, the environment impedance will feel like  $E$  scaled by the ratio  $n_f/n_p$ , while the slave feels  $H$  by the inverse ratio. It was shown that a local feedback could occur in the slave to change its apparent mass but a similar feedback could just as easily be used to make the master’s apparent mass different. These equations demonstrate that our ideal teleoperation can be achieved for  $n_p$  and  $n_f$  chosen independently by applying (5); however, for transparency in which the apparent master and slave device properties do not differ from their actual ones, we require  $n_f = n_m n_p$ .

Although these equations involve rigid bodies in free space, more general plant models can similarly be manipulated for perfect transparency. Of course, ideal teleoperation is impossible due to time delays, modeling errors,

measurement noise, *etc.*. Using a controller with only force measurements as in (5) would also result in a loss of kinematic correspondence between master and slave. These are the reasons why bilateral controller design is necessary and nontrivial.

## II. $H_\infty$ DESIGN APPROACH

In 1981, Zames introduced the concept of  $H_\infty$  control as a method of synthesizing a controller to minimize the sensitivity of a simple single-input, single-output (SISO) system [27]. Since then, the field of  $H_\infty$ -optimal control has grown tremendously and is widely recognized for its theoretical and practical use in synthesizing and analyzing controllers.

The  $\infty$ -norm of a real-rational transfer matrix  $G(s)$  is defined as its maximum singular value  $\bar{\sigma}$  over all frequencies.

$$\|G\|_\infty := \sup_{\omega \in \mathbb{R}} \bar{\sigma}(G(j\omega)) \quad (7)$$

Essentially, it places a bound on the output signal in the following sense: if  $y = Gu$  then  $\|y\|_2 \leq \|G\|_\infty \|u\|_2$  (for a real, vector-valued signal  $x(t)$ ,  $\|x\|_2 = [\int_{-\infty}^{\infty} x^T(t)x(t)dt]^{1/2}$ ).

### Standard Problem

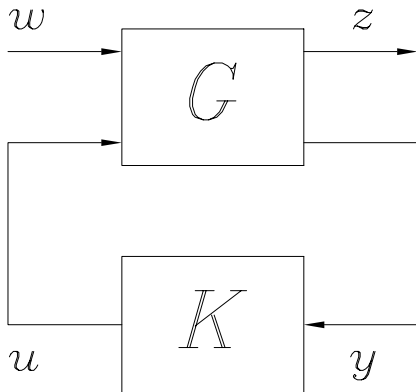


Fig. 5. Standard  $H_\infty$  Problem

Consider the block diagram in Figure 5. There are four vector-valued signals of interest: the plant exogenous inputs  $w$  (*e.g.*, reference signals, disturbances, measurement noise, *etc.*), the error outputs  $z$  to be minimized (*e.g.*, tracking errors, weighted actuator outputs, *etc.*), the compensator control signals  $u$  and the measurements  $y$  used in the control law. The plant  $G$  and controller  $K$  are assumed to be systems which can be mathematically represented by proper, real-rational transfer matrices. Frequency dependent weighting functions which characterize the desired behavior are assumed to be absorbed in the plant  $G$  (*e.g.*, for reducing sensitivity to disturbances or for increasing robustness to plant uncertainties).

The plant  $G$  can be partitioned as

$$G(s) = \begin{bmatrix} G_{11}(s) & G_{12}(s) \\ G_{21}(s) & G_{22}(s) \end{bmatrix}. \quad (8)$$

For a given compensator  $K$ , the resulting closed-loop transfer function matrix mapping  $w$  to  $z$  is given by

$$T_{zw} = G_{11} + G_{12}K(I - G_{22}K)^{-1}G_{21}. \quad (9)$$

The standard  $H_\infty$ -optimization problem is to find a realizable controller  $K$  which stabilizes  $G$  and minimizes  $\gamma$  such that  $\|T_{zw}\|_\infty < \gamma$  ( $\gamma$  is the upper bound on the norm). Design for the  $H_\infty$  criterion corresponds to designing for the worst-case expected exogenous signal. The analytical and numerical solution to this problem is nontrivial because it may not exist or may not be unique. However, numerous algorithms are available to solve the standard  $H_\infty$  problem when it is well-posed [28], [29], [30].

Although  $H_\infty$  control was originally introduced for shaping the system sensitivity function  $\tilde{S}(s)$  to provide good performance, it can just as easily be used for its dual, the complementary sensitivity function  $\tilde{T}(s)$ , to provide robustness (the tilde is used to distinguish the sensitivity function from the scattering operator and the complementary sensitivity function from other transfer functions). That is to say, instead of minimizing the norm of the weighted sensitivity  $\|W_1\tilde{S}\|_\infty$ , one could choose to minimize  $\|W_2\tilde{T}\|_\infty$ . Now with the  $H_\infty$  approach, it is possible to combine these two and minimize a single norm defined by:

$$\left\| \begin{bmatrix} W_1\tilde{S} \\ W_2\tilde{T} \end{bmatrix} \right\|_\infty \quad (10)$$

This is described as the ‘‘Mixed-Sensitivity Approach’’ in [31], but is more commonly known as the ‘‘Robust Performance Problem’’ [32]. Because of the relationship between  $\tilde{S}(s)$  and  $\tilde{T}(s)$  (*i.e.*, their sum must be unity), there is an inherent tradeoff and one can only be minimized at the expense of the other. The practical solution is to minimize  $\tilde{S}(s)$  at low frequencies where the model is more accurate and performance is more important, and then minimize  $\tilde{T}(s)$  at high frequencies where there is more uncertainty and robustness is necessary. This is done by choosing  $W_1(s)$  to be low-pass and  $W_2(s)$  to be high-pass. From a practical standpoint, it is also important to limit the control signal and this can be achieved by including it as an output. The  $H_\infty$  approach is to minimize the norm of the transfer matrix mapping the input to a vector with all three of these signals, properly weighted. The relative magnitudes of  $W_1$  and  $W_2$  can be used to tradeoff the performance versus robustness. For example, if it is found that performance is not good enough at a certain frequency then  $W_1$  should be increased in that region while if instability is occurring, then  $W_2$  should be increased.

### Modelling and Synthesis

In [28], Doyle *et al.* showed that  $H_\infty$  (sub)optimal controllers exist *iff* the unique stabilizing solutions to a pair of associated Riccati equations exist, are positive definite, and the spectral radius of their product satisfies an upper bound criterion. The Matlab Robust Control Toolbox [31] uses a ‘‘loop-shifting two-Riccati’’ algorithm to calculate an  $H_\infty$  controller with the option of performing a binary iteration to find the optimal, to achieve the goal:

$$\left\| \begin{bmatrix} T_{zw}(\phi) \\ T_{zw}(\bar{\phi}) \end{bmatrix} \right\|_\infty \leq 1, \quad (11)$$

where the designer specifies the set of output indices  $\phi$  on which the iteration is to be performed. The other indices  $\bar{\phi}$

are not scaled either because they cannot (*e.g.*, once the actuator limitations are known, the saturation signals cannot be altered) or the particular error signal is not too significant (*e.g.*, if the position tracking is only required to be within a certain range but force tracking should be optimized, then the iteration would be performed on the force error but not the position error). This is consistent with the two different viewpoints on weightings which are that they may be fixed quantities not subject to manipulation by the designer or that they are parameters chosen by the designer to allow different criteria to be traded off. If a solution for which  $\gamma < 1$  is found, then the requirements are too strict and the weighting function for the indices in  $\phi$  need to be reduced by a factor of  $\gamma$ ; similarly, if  $\gamma > 1$ , then tighter requirements can be made by increasing the weighting function for the indices in  $\phi$  by  $\gamma$ .

With regard to  $H_\infty$ -based controllers, a reasonable measure of performance is the  $\infty$ -norm of the resulting closed-loop transfer function,  $\|T_{zw}\|_\infty$ ; this norm is desired to be as small as possible for a given plant. This approach allows specification for performance and robustness in a single measure simply by including the associated transfer functions in the closed-loop plant. It might even be argued that a properly specified plant will allow the designer to quickly assess how well the controller meets the specifications. The reference value for the  $\infty$ -norm then is unity so if  $\gamma < 1$ , the controller can meet the design goals and if  $\gamma > 1$ , it cannot. One might also contend that if  $\gamma$  is not close to unity, then the plant may have been poorly specified because careful consideration of the system dynamics and limitations should allow a reasonable choice of weightings; however, if the designer had this much insight, then  $H_\infty$  theory might not even be necessary for the optimization! It is instructive to consider the relationship between  $\gamma$ ,  $\beta$ , and  $\gamma$ . If the optimizing iteration procedure is to be performed on all the output indices, then the optimal  $\beta$  is equivalent to  $\gamma^{-1}$ .

The general structure of the model in our framework appears in Figure 6.  $P_m$  and  $P_s$  are the master and slave plants, respectively,  $f_h$  is the operator hand force which can be decoupled into an active part  $f_{ha}$  and a passive part  $f_{hp}$ , and similarly, the environment force  $f_e$  can be decoupled into  $f_{ea}$  and  $f_{ep}$ . The applied actuator and the net forces on the master and slave are, respectively,  $f_{ma}$ ,  $f_{sa}$ ,  $f_m$  and  $f_s$ , while the output master and slave positions are, respectively,  $x_m$  and  $x_s$ . Measurement noise in the force and position signals can be represented by the vector  $v_2 = [n_{fm} \ n_{fs} \ n_{pm} \ n_{ps}]^T$  which result in the measurement signal used in the compensator  $y = [\tilde{f}_h \ \tilde{f}_e \ \tilde{x}_m \ \tilde{x}_s]^T$ . Disturbances are represented by the vector  $v_1 = [d_{cm} \ d_{cs}]^T$  which alter the commanded actuator forces  $u = [f_{ma} \ f_{sa}]^T$ .  $W_T$  represents a time delay, and finally,  $K$  represents the compensator which is to be designed.

Before proceeding further, some remarks about this structure should be made to clarify points of possible confusion:

1. The time delay  $W_T(s) = e^{-sT}$  is infinite-dimensional

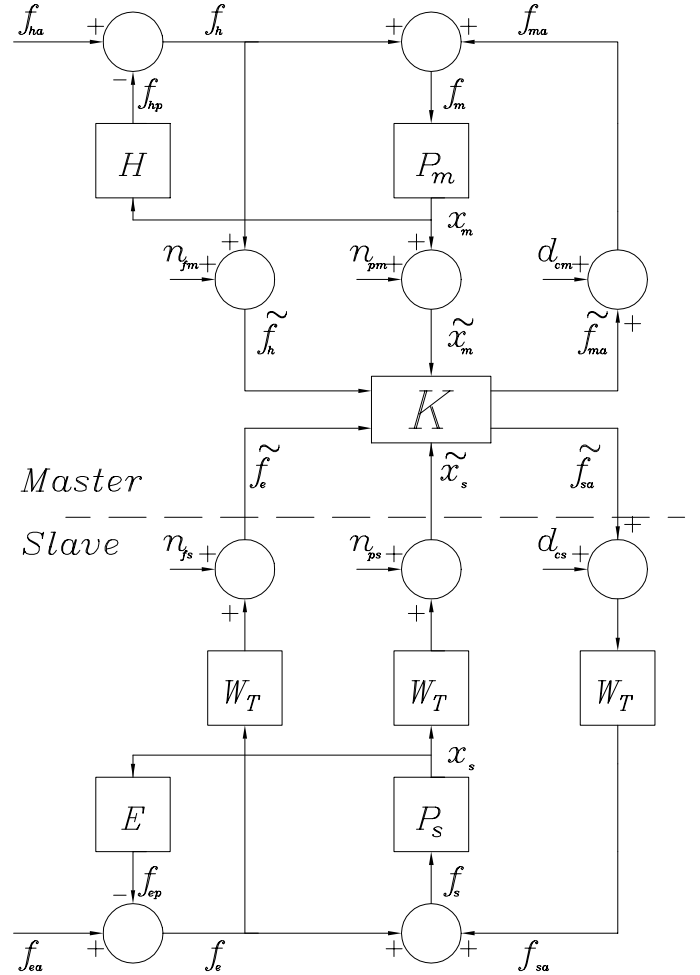


Fig. 6. Framework for Controller Synthesis

in polynomial space and cannot be represented exactly in the model. A Padé all-pass approximation of arbitrarily high order can be made for  $W_T$  using the MacLaurin series expansion:

$$e^{-sT} = \frac{e^{-sT/2}}{e^{sT/2}} = \frac{1 - sT/2 + (sT)^2/8 - (sT)^3/48 + \dots}{1 + sT/2 + (sT)^2/8 + (sT)^3/48 + \dots} \quad (12)$$

Approximations using a truncation of this series are most valid at low frequencies and if other frequencies are of interest then a more general Taylor series expansion about a different value might be used.

2.  $W_T(s)$  has only been added to the slave side to consider the case of remote teleoperation in which the controller is on the master's side. It would be just as easy, but unlikely necessary, to model such delays on the master side.
3. Even in the simplest 1-DOF case, the teleoperation problem is multi-input, multi-output (MIMO) because the minimum require inputs are  $f_h$  and  $f_e$ , and the minimum outputs involve tracking of the forces and positions.
4.  $P_m$  and  $P_s$  are assumed to be the resulting transfer functions after the use of local controllers to stabilize each manipulator. For example, in our experiments,

local PD controllers have been used so that  $P_m = 1/(m_m s^2 + b_m s + k_m)$  and  $P_s = 1/(m_s s^2 + b_s s + k_s)$ . Here,  $P_m$  and  $P_s$  are assumed to be given but, more generally, their local controllers might need to be designed for a particular task (*e.g.*, choose them according to the functions  $E$  and  $H$ ).

5. The disturbances here are assumed to be at the compensator outputs (or equivalently at each manipulator input) which can be interpreted as random forces or torques acting on the arms or uncertainties in the compensator, perhaps due to calibration error or discretization of the output signals. Although not shown in the figure, disturbances can also be at the outputs of the manipulators. By including disturbances in the model, robustness to model uncertainties can be increased.
6. The model shown in Figure 6 only applies to rigid manipulators, since the actuator forces and forces due to the dynamic interaction with the environment or hand enter the slave and master plants at the same point. However, it is relatively straightforward to extend the approach to plant models that account for link or joint flexibility. For example,  $x_m = P_m f_m$  can be replaced with  $x_m = P_{ma} f_{ma} + P_{mh} f_h$  on the master side, with the transfer functions  $P_{ma}$  and  $P_{mh}$  determined from the master manipulator model.

The designer is left to decide which error signals to minimize and how to weigh them to provide the desired behavior. The difficulty is that there is a great deal of freedom in these choices and it may seem rather arbitrary how this is done. As an example, a possible set of outputs to minimize is as follows:

- $z_1 = W_1(f_{ma} - n_f W_T f_e)$ : The master actuator force should track the delayed environment force (since the presence of the delay makes instantaneous tracking impossible), scaled by a specified force-scaling ratio  $n_f$ . This is a performance requirement which is important at lower frequencies so  $W_1$  is chosen to be low-pass. Minimization of this signal might be described as “maximizing the force transparency at the master”.
- $z_2 = W_2(x_s - W_T P_m(f_h + n_f W_T f_e)/n_p)$ : The slave position should track the delayed motion of the “expected” master motion scaled by a specified position scaling ratio  $n_p$ . It is “expected” because it depends on the forces  $f_h$  and  $f_e$  but does not include  $f_{ma}$ . Again, this is a performance requirement and  $W_2$  is chosen to be low-pass. Minimization of this signal might be described as “maximizing the position transparency at the slave”.
- $z_3 = W_3(x_m - n_p x_s)$ : Kinematic correspondence between the master and slave should be maintained. This signal is similar to  $z_2$  and, in fact, they are essentially equivalent when  $z_1$  is perfectly optimized (*i.e.*,  $f_{ma} = n_f W_T f_e$ ) and there is no time delay.  $W_3$  is chosen to be low-pass.
- $z_4 = W_4 \hat{f}_{ma}$ :  $W_4$  is chosen to be high-pass. This serves the dual purpose of accounting for master actuator

saturation at high frequencies and improving robustness by having the controller output roll off at high frequencies [33].

- $z_5 = W_5 \hat{f}_{sa}$ :  $W_5$  is chosen to be high-pass for the slave actuator using the same reasoning as for  $W_4$ .

The redundancy between  $z_2$  and  $z_3$  can be eliminated by ignoring one of them; another option is to design a more symmetric controller by changing  $z_2$  to maximize the force transparency at the slave. The weighting functions  $W_{f_m}, W_{f_s}, W_{p_m}, W_{p_s}, W_{c_m},$  and  $W_{c_s}$  describe the frequency spectrums in the noise signals  $n_{f_m}, n_{f_s}, n_{p_m},$  and  $n_{p_s}$  and disturbance signals  $d_{c_m},$  and  $d_{c_s}$ , respectively (*i.e.*,  $n_{(\cdot)} = W_{(\cdot)} \hat{n}_{(\cdot)}$  for  $\|\hat{n}_{(\cdot)}\|_2 \leq 1$  and  $d_{(\cdot)} = W_{(\cdot)} \hat{d}_{(\cdot)}$  for  $\|\hat{d}_{(\cdot)}\|_2 \leq 1$ ). With the choice of  $z$  made, the model can be transformed into the standard problem.

Define the signals as  $w = [f_{ha} \ f_{ea} \ \hat{n}_{f_m} \ \hat{n}_{f_s} \ \hat{n}_{p_m} \ \hat{n}_{p_s} \ \hat{d}_{c_m} \ \hat{d}_{c_s}]^T$ ,  $y = [f_h + n_{f_m} \ W_T f_e + n_{f_s} \ x_m + n_{p_m} \ W_T x_s + n_{p_s}]^T$ ,  $u = [\hat{f}_{ma} \ \hat{f}_{sa}]^T$  and  $z = [z_1 \ \dots \ z_5]^T$ . The plant is then described by

$$G = \begin{bmatrix} W_{out} G'_{11} W_{in} & W_{out} G'_{12} \\ G_{21} W_{in} & G_{22} \end{bmatrix} \quad (13)$$

where

$$\begin{aligned} \begin{bmatrix} z \\ y \end{bmatrix} &= G \begin{bmatrix} w \\ u \end{bmatrix} \\ W_{in} &= \text{diag}\{1, 1, W_{f_m}, W_{f_s}, W_{p_m}, W_{p_s}, W_{c_m}, W_{c_s}\} \\ W_{out} &= \text{diag}\{W_1, W_2, W_3, W_4, W_5\} \end{aligned}$$

and  $G'_{11}, G'_{12}, G_{21}$  and  $G_{22}$  are defined in (14, 15, 16, 17) below with  $P_{mH} = \frac{P_m}{1+P_m H}$  and  $P_{sE} = \frac{P_s}{1+P_s E}$  introduced for notational convenience.  $W_{in}$  represents the weightings at the plant inputs (weighting functions might have been used in place of unity on the exogenous force signals to reflect their expected spectrums) and is less subject to design than  $W_{out}$  which represents the weightings at the specified outputs. It should be recognized that for the SISO case, it does not matter if the weighting is considered at the input or output but for the MIMO case, the choice is more important; for example, the poles of a weighting function used at one input will show up in the transfer function of that input to every output but if it is used at an output, it exists in transfer functions for every input signal to only that output.

The plant  $G$  can easily be reduced to simpler models. For example, (i) to ignore the time delay, set  $W_T = 1$ ; (ii) if no force/torque (F/T) sensing is available, remove rows 6 and 7 and columns 3 and 4; (iii) to ignore the passive feedback, set  $E = H = 0 \Rightarrow P_{mH} = P_m, P_{sE} = P_s$ ; (iv) for identical master and slave with unity scaling, set  $P_m = P_s$  and  $n_p = n_f = 1$ ; and (v) to ignore the actuator saturations, remove rows 3 and 4. This is demonstrated in the design example presented in Section III. An interesting observation is that when the plant has no time delays, measurement noise or disturbances and the actuators do

$$G'_{11} = \begin{bmatrix} 0 & \frac{-n_f W_T}{1+P_s E} & 0 & 0 & 0 & 0 & 1 & n_f E P_s E W_T^2 \\ -\frac{W_T P_{mH}}{n_p} & \frac{P_s - W_T^2 P_m n_f / n_p}{1+P_s E} & 0 & 0 & 0 & 0 & \frac{W_T P_m H P_{mH}}{n_p} & P_s E W_T \left(1 + \frac{n_f P_m E P_s E W_T^3}{n_p}\right) \\ P_{mH} & -n_p P_s E & 0 & 0 & 0 & 0 & P_{mH} & -n_p P_s E W_T \\ 0 & 0 & 0 & 0 & 0 & 0 & 0 & 0 \\ 0 & 0 & 0 & 0 & 0 & 0 & 0 & 0 \end{bmatrix} \quad (14)$$

$$G'_{12} = \begin{bmatrix} 1 & n_f E P_s E W_T^2 \\ \frac{W_T P_m H P_{mH}}{n_p} & P_s E W_T \left(1 + \frac{n_f P_m E P_s E W_T^3}{n_p}\right) \\ P_{mH} & -n_p P_s E W_T \\ 1 & 0 \\ 0 & 1 \end{bmatrix} \quad (15)$$

$$G_{21} = \begin{bmatrix} \frac{1}{1+P_{mH}} & 0 & 1 & 0 & 0 & 0 & -H P_{mH} & 0 \\ 0 & \frac{W_T}{1+P_s E} & 0 & 1 & 0 & 0 & 0 & -W_T^2 E P_s E \\ P_{mH} & 0 & 0 & 0 & 1 & 0 & P_{mH} & 0 \\ 0 & W_T P_s E & 0 & 0 & 0 & 1 & 0 & W_T^2 P_s E \end{bmatrix} \quad (16)$$

$$G_{22} = \begin{bmatrix} -H P_{mH} & 0 \\ 0 & -W_T^2 E P_s E \\ P_{mH} & 0 \\ 0 & W_T^2 P_s E \end{bmatrix} \quad (17)$$

not saturate, then the ideal control law (5) ensures perfect tracking of the first three outputs (*i.e.*, the  $\infty$ -norm from  $[f_{ha} \ f_{ea}]^T$  to  $[z_1 \ z_2 \ z_3]^T$  is identically zero); this is not surprising and it supports the assertion that minimization of the first three outputs is equivalent to optimizing transparency and performance.

A modification of the presented framework might also allow the designer to include a passivity measure of the teleoperation system. This can be achieved by using wave variables ( $f+v$ ) and ( $f-v$ ), instead of the forces  $f = [f_h \ f_e]^T$  and velocities  $v = [v_m \ v_s]^T$  in the formulation of Figure 6. Recall that a system with scattering matrix  $S(s)$ , where  $f-v = S(s)(f+v)$ , is passive *iff*  $\|S\|_\infty \leq 1$  [10]. Thus, by adding an exogenous disturbance to ( $f+v$ ) and including ( $f-v$ ) as an unweighted output, system passivity would be insured if the resulting  $\gamma$  is subunity. The compensator derived using the above modification takes in measurements of the wave variables (( $f+v$ ) and ( $f-v$ )) but it can be transformed back to take in measurements of force and velocity. For most motion-scaling systems, including the example described in this paper, the desired effect often requires power amplification and therefore cannot be passive [10], [18]. However, if one was willing to trade off tracking of either force or position, a solution to the problem should exist. As an example, consider a teleoperator which emulated a pair of forceps to provide force and position scaling. The system would be passive and provide the desired downward motion-scaling, but there would be none of the desired force magnification so such an emulation would defeat the purpose of the force-reflection in the teleoperator. Another solution to the problem is to minimize  $\gamma$  instead of requiring it to be strictly less than one; this minimizes the scattering matrix norm which, in turn, increases the stability margin. A less conservative approach

is to somehow incorporate the  $\mu$ -synthesis methodology as in [18], [19]. These are all areas for future research.

### Controller Characteristics

At this point, it is worth pointing out some characteristics of this approach paying particular attention to how general it is. The problem has been cast in an  $H_\infty$  framework which works well for MIMO systems. In such a framework, the designer works directly with the closed-loop transfer function. There are a number of solutions for standard  $H_\infty$  problems and some other concepts, such as the parameterization of all stabilizing compensators, should prove useful.

There is no assumption that the environment is passive as in many papers. Both the human and environment can be systems applying active exogenous force signals. If a stabilizing  $K$  can be found, then the stability is guaranteed because the work deals directly with the closed-loop system. However, if one chooses to assume a passive environment, then there is also a method to guarantee passivity of the teleoperator by involving wave variables in the model.

The signals of interest here are forces and positions. Other approaches often adopt velocities instead of positions and there are two reasons this might be done; firstly, forces and velocities can be used together in passivity theory, and secondly, the mapping from force to velocity has a single pole but the mapping to position has a double pole. Intuitively, the position signal is more important and velocity stability does not guarantee position stability. As well, all the force and position measurements are utilized in the controller and there is no restriction on the order of their gains making it one of the most general architectures compared to others in the literature.

A multiple of control objectives can be simultaneously



frequency actuator gains. Performance *vs* robust stability tradeoffs are achieved by manipulating the weights in the above equation. It should be remembered that the bandwidths for the actuators must be higher than those for both the force and position tracking so that control signals can be applied to optimize them. As well, human asymmetrical input/output capabilities indicate that the force transparency bandwidth should be higher than that for kinematic correspondence [25]. The weighting functions should reflect these qualities. For example, for the kinematic correspondence, the designer might want the error to be low for frequencies below 10 rad/s but allow errors above 40 rad/s to be as much as 10 times higher; the weighting could then be chosen to be  $W_2(s) = \frac{(s+40)^2}{(s+10)^2}$ . Similar reasoning could be used to choose the other weightings. The ones used are  $W_1(s) = \frac{0.01(s+100)^2}{(s+25)^2}$ ,  $W_2(s) = \frac{(s+40)^2}{(s+10)^2}$ ,  $W_3(s) = \frac{0.07(s+60)}{(s+150)}$ , and  $W_4(s) = \frac{0.5(s+55)}{(s+125)}$ .

To determine the measurement noise weightings, both wrists were deactivated and their position signals were stored. A spectrum analysis of these signals revealed that the noise was not concentrated in any specific frequency range so for simplicity, the noise weighting signals were chosen to be constants of the largest components seen:  $W_{pm} = 2.5\mu\text{m}$  and  $W_{ps} = 1\mu\text{m}$ ; in reality, the high frequency uncertainty is expected to be quite high and this should be represented in the weightings. A similar analysis might have been performed on the outputs from the current drivers to determine the spectrum of disturbance signals expected but this was not done as stable performance was achieved with the simple assumption of low frequency disturbances of magnitude 1 mN in the microwrist (calculated as the highest force resolution using the present hardware) and 10 mN in the macrowrist (the weighting spectrums assumed are  $W_{cm} = \frac{0.01}{s+1}$  and  $W_{cs} = \frac{0.001}{s+1}$ ).

The motion and force-scaling ratios were selected to be  $n_p = 10$  and  $n_f = 40$ , respectively. The model of the plant then becomes

$$G = \begin{bmatrix} W_{out}G'_{11}W_{in} & W_{out}G'_{12} \\ G_{21}W_{in} & G_{22} \end{bmatrix} \quad (20)$$

where

$$\begin{bmatrix} z \\ y \end{bmatrix} = G \begin{bmatrix} w \\ u \end{bmatrix}$$

$$W_{in} = \text{diag}\{1, 1, W_{pm}, W_{ps}, W_{cm}, W_{cs}\}$$

$$W_{out} = \text{diag}\{W_1, W_2, W_3, W_4\}$$

$$G'_{11} = \begin{bmatrix} 0 & \frac{-n_f}{1+P_sE} & 0 & 0 & 1 & n_fEP_sE \\ P_{mH} & -n_pP_sE & 0 & 0 & P_{mH} & -n_pP_sE \\ 0 & 0 & 0 & 0 & 0 & 0 \\ 0 & 0 & 0 & 0 & 0 & 0 \end{bmatrix}$$

$$G'_{12} = \begin{bmatrix} 1 & n_fEP_sE \\ P_{mH} & -n_pP_sE \\ 1 & 0 \\ 0 & 1 \end{bmatrix}$$

$$G_{21} = \begin{bmatrix} P_{mH} & 0 & 1 & 0 & P_{mH} & 0 \\ 0 & P_sE & 0 & 1 & 0 & P_sE \end{bmatrix}$$

$$G_{22} = \begin{bmatrix} P_{mH} & 0 \\ 0 & P_sE \end{bmatrix}$$

In the following examples, a nominal controller is synthesized, and then it is shown how one might try to improve different performance criteria, improve robustness, and account for human and environment impedances.

### Nominal Free Motion Tracking

For this first example, the impedances will be set to zero (*i.e.*,  $H = E = 0$ ). This choice considers that each wrist might be in free motion and simplifies the plant to be controlled (some of the elements vanish and others have lower order). This plant has an order of almost 40 but for the synthesis, the Matlab balanced model reduction function “balmr” was used to reduce it to 10. By performing the  $\mu$ -iteration on the first two outputs, a controller was found with the parameter  $\kappa_1 = 0.320$ , implying that in the worst case, the error signals may be as much as three times larger than the performance specifications; this controller will be designated as  $\kappa_1$ . The resulting continuous-time controller gains from each input are strictly proper transfer functions. The closed-loop responses for the unaugmented plant (*i.e.*, without the weighting functions) are shown in Figure 8 for the master force input (the responses to each noise and disturbance input are not as important and do not provide much more insight into the design so they are not shown).

Using the designed  $H_\infty$  controller, simulations of the system showed reasonably good position tracking but the master actuator force tracked roughly more than 20 times the slave environment force instead of the specified 40 times; however, this does not conflict with the plant model because the force transparency weighting was specified to be less important than the position tracking (notice that  $W_1(0) = 0.16$ , implying the DC response might be off by as much as 600% in the specifications). It should also be noted that a discretized state-space controller was used in the simulation to more accurately describe the system in the experiments.

For the experiments, the state-space controller was discretized for a sampling period of 5 ms using a Tustin approximation. The “feel” was reasonably good and some experimental results are shown in Figure 9 (the F/T sensors have not yet been mounted on the wrist fltors so the exogenous forces cannot be displayed). In (a), the master was randomly driven by hand with the slave in free motion and in (b), the roles were reversed.

### Trading Off Different Performance Criteria

Consider now that the designer may want better force tracking. The simplest way to do this is to change the weighting  $W_1$  to be larger in the frequency range of interest. For simplicity,  $W_1$  was made four times larger and the synthesis was repeated. A new controller,  $\kappa_2$ , was obtained with the parameter  $\kappa_2 = 0.082$ . It is interesting to note here that  $\kappa_2$  decreased by almost as much as  $W_1$  was increased, indicating that there may be no significant improvement in the force tracking but the position tracking may be four times as bad. Only the Bode plots for the force and position tracking responses are important and these are shown in Figure 10. When compared to the closed-loop responses

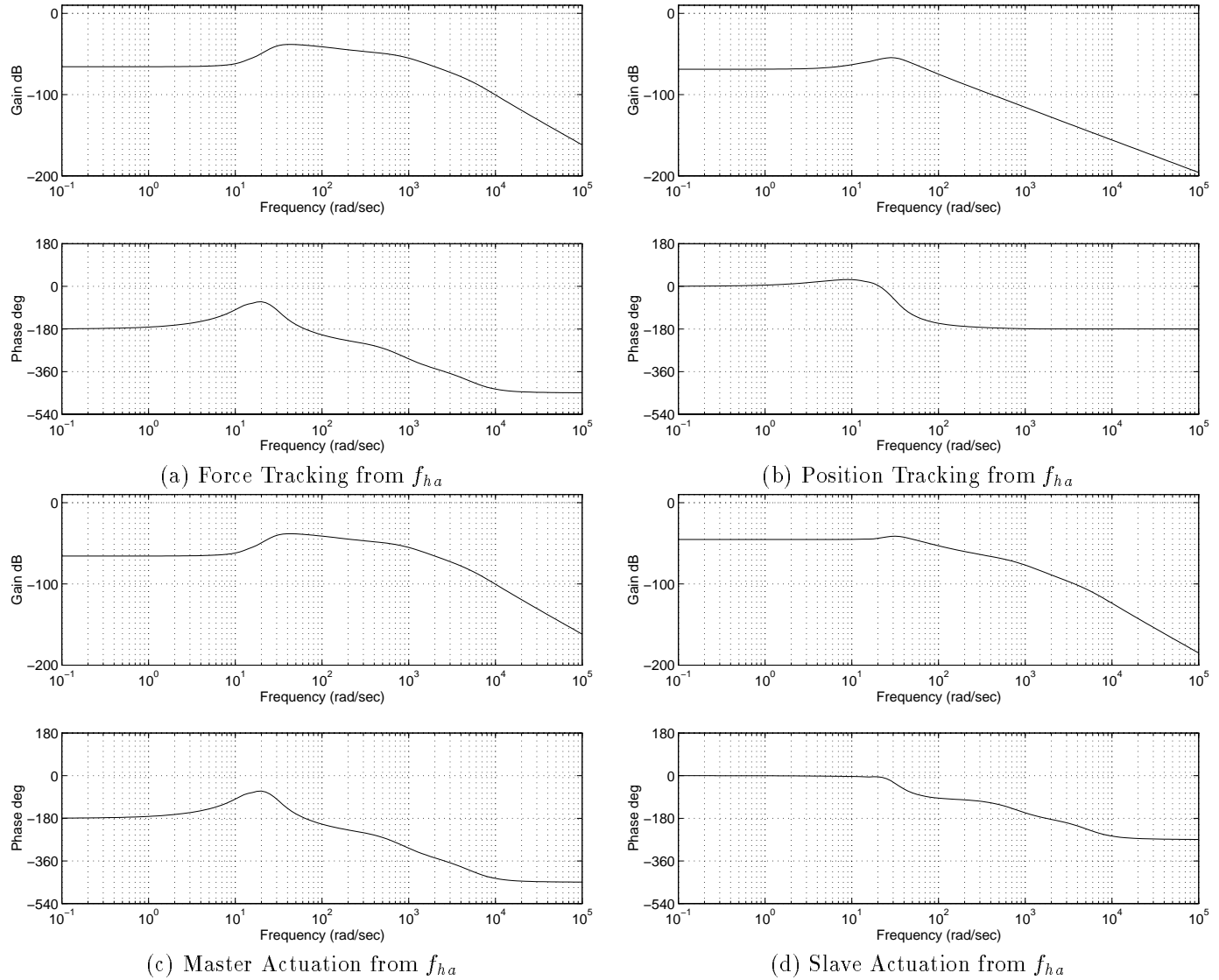


Fig. 8. Closed-Loop Responses to Exogenous Forces for Controller  $\kappa_1$

of controller  $\kappa_1$  in Figure 8, it is seen that the new force tracking is actually worse at low frequencies but becomes better for frequencies above 200 rad/s or 32 Hz; the position tracking is also worse at low frequencies but is relatively unchanged for high frequencies. Thus, slightly better high frequency force tracking was achieved at the expense of low frequency tracking of both position and force. It is likely that the reason no significant improvement in the force tracking could be made is that the performance in controller  $\kappa_1$  was already close to the limitations given the assumed disturbances and actuator limitations. Experiments with the controller  $\kappa_2$  showed that the transparency perceived by the operator is worse, as expected because the manipulation at low frequencies is much poorer.

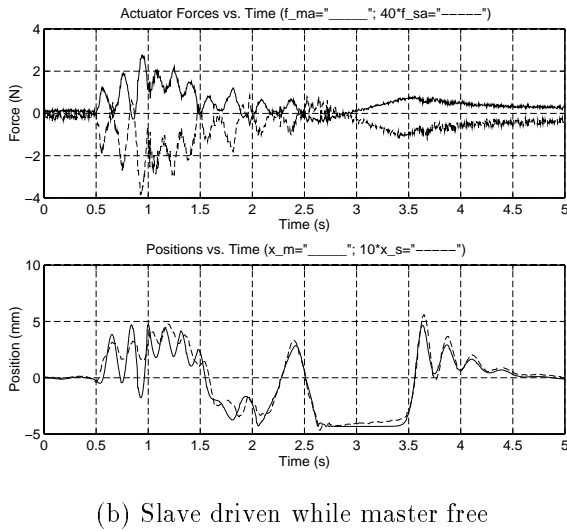
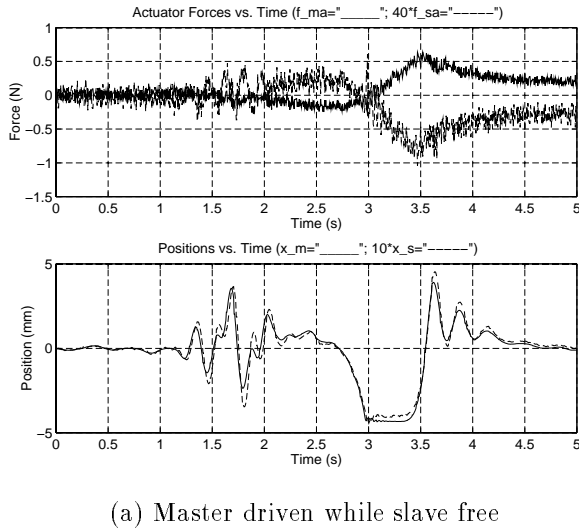
### Trading Off Performance and Robustness

In the last section, it was mentioned that the force transparency may be limited by the assumptions on disturbances and actuation. Now consider how one might sacrifice some robustness to get better performance. For example, consider the original plant but assume no force disturbances

and that the actuator limitations are only half of what they originally were (*i.e.*,  $W_{cm} = W_{cs} = 0$ ,  $W_3 = \frac{0.035(s+60)}{(s+150)}$  and  $W_4 = \frac{0.25(s+55)}{(s+125)}$ ). The controller synthesized here,  $\kappa_3$ , had a parameter value  $\gamma = 2.4$  implying that the error specifications could be made tighter if desired. The Bode plot responses for this controller are shown in Figure 11 indicating that force and position tracking will be improved. It can be shown that this tracking improves at the expense of poor rejection of high frequency disturbances [7].

Simulations using  $\kappa_3$ , compared to those using  $\kappa_1$ , revealed much higher frequency components in the actuation forces and much better force and position tracking (the force tracking is indeed closer to the originally specified forty times). Experimentation with the new controller is shown in Figure 12. The higher frequency actuation components expected were observed and, as evidenced by oscillations, the system was unstable when neither manipulator was held.

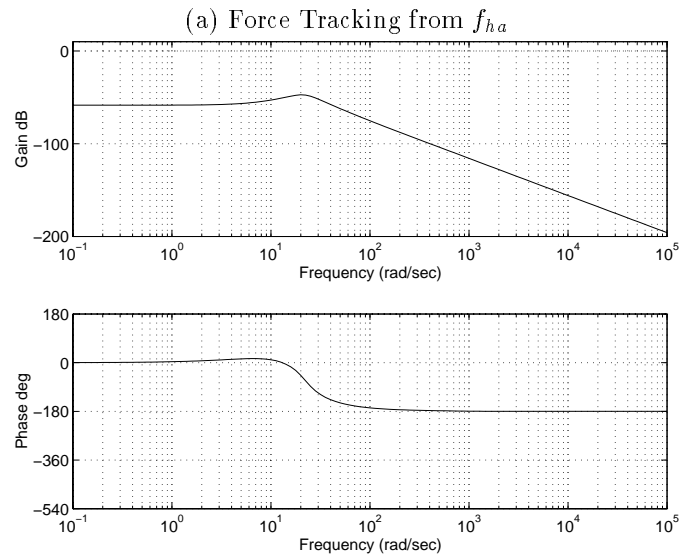
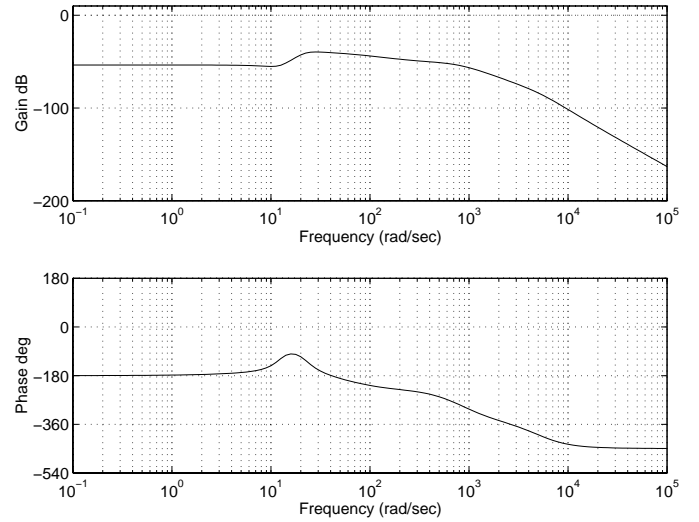
Alternatively, if greater robustness was required, the de-

Fig. 9. Experiment for  $\kappa_1$ : Free Motion Tracking

signer could assume larger disturbances. Controller  $\kappa_4$  was synthesized by assuming disturbances at the master and slave that were ten times their original values and the parameter was  $\gamma = 0.25$ . Figure 14 shows experiments using  $\kappa_4$  and can be compared to Figure 9. Slave disturbances have a smaller effect and the system is more robust. With regard to performance, less transparency is experimentally evident from a more sluggish feel.

### Hard Contact

Hard contact is known to be a problem in controlling manipulators because of the highly discontinuous nature of the task. Instability was found in simulations using controller  $\kappa_1$  when a stiff environment impedance was suddenly introduced. To overcome this, an impedance model of the environment as a spring was included in the plant. A relatively small value of  $E = 10$  N/m was assumed and the resulting controller,  $\kappa_5$ , had a  $\gamma$  value of 0.402. Simulations of this controller showed that the system remains stable for impedances even larger than 3000 N/m (similar simulations using  $\kappa_1$  were unstable for impedances as low as 50 N/m). A problem with the synthesis and simulation

Fig. 10. Tracking Responses for Controller  $\kappa_2$ 

is that constant contact with the environment is assumed but the discontinuous forces expected in experiments would likely make things worse. As well, stability is not guaranteed for free motion. It may be possible to model the environment impedances as uncertainties to remedy this.

As expected, controller  $\kappa_1$  exhibited stability problems in hard contact experimentally as seen in Figure 15(a). Here, both wrists were left in free motion and a rigid metal surface was brought to the edge of the slave flotor edge and stiffly held there, resulting in instability. The modified controller designed for contact with the environment was implemented and successful in achieving stability under the same conditions (see Figure 15(b)). Thus, even some estimate of the impedance is expected to improve stability.

Only experimental results have been presented but simulations of the above designs were also performed. It is interesting to note that the inclusion of a stiff environment impedance model significantly increases the controller term corresponding to local force-feedback at the slave. This coincides with common practice as discussed, for example, in

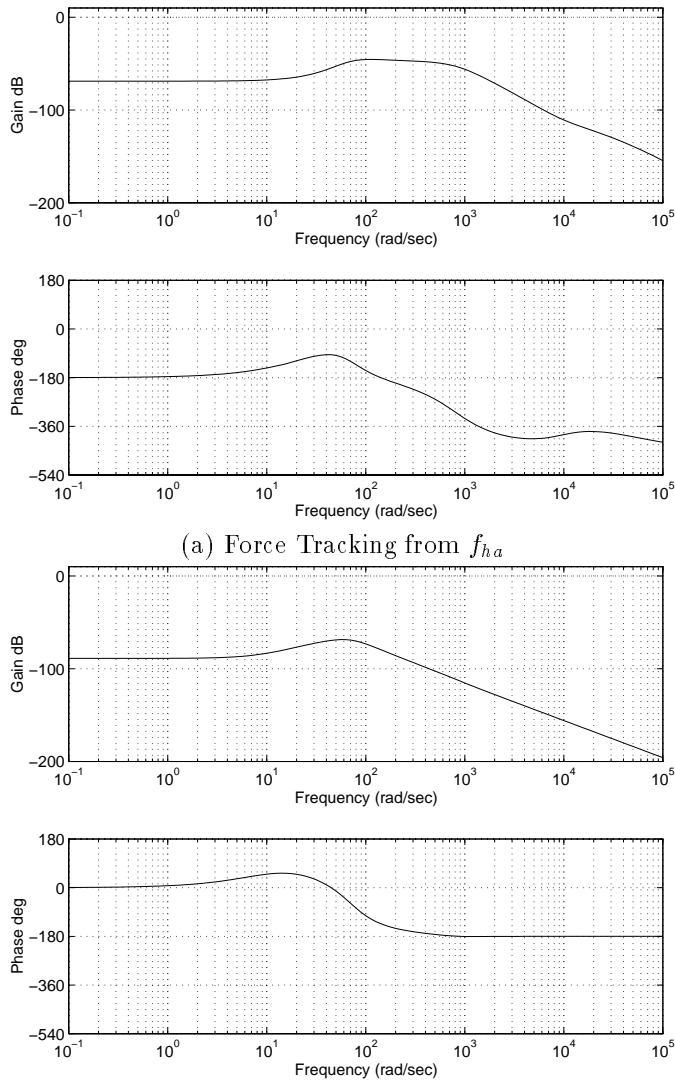


Fig. 11. Tracking Responses for Controller  $\kappa_3$

[10].

#### IV. CONCLUSIONS

Aspects of bilateral controller design for teleoperation systems have been presented. A very general  $H_\infty$  framework for trading off various performance criteria and robustness has been described. Experiments demonstrate that such an approach leads to practical and effective controller designs. More details on the simulations and experiments can be found in [7]. As well, systems designed with a first order approximation of time delays did show greater robustness to delays but they have not yet been analysed rigorously for presentation.

There is much future work to continue on this controller design strategy. The manipulators are being instrumented with 6-axis F/T sensors; experimentally, the motion-scaling controller works well even when based only on position sensing but force sensing is anticipated to significantly improve the performance, especially during contact tasks. The effect of model reduction and discretiza-

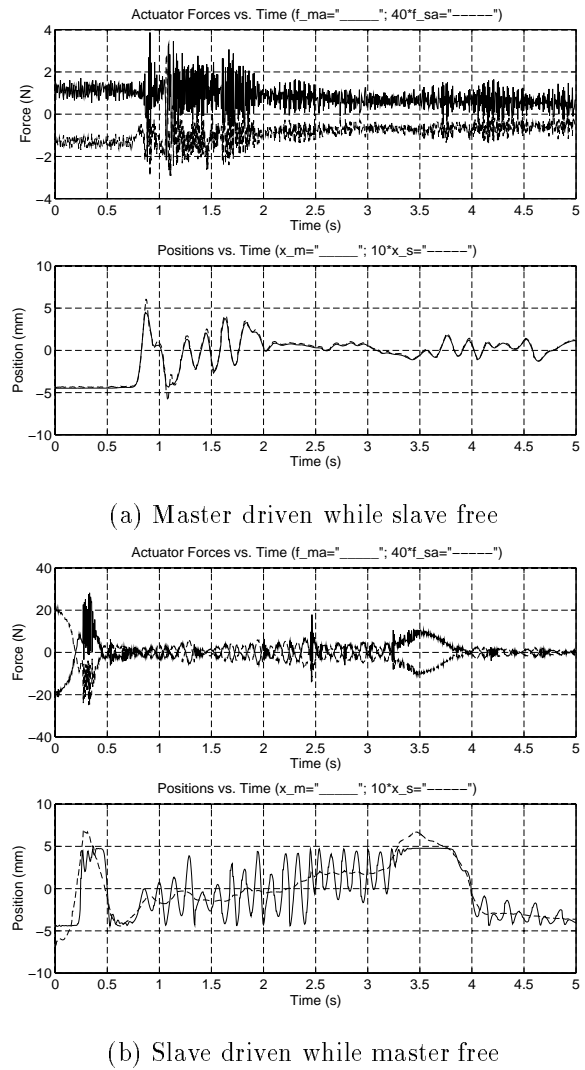
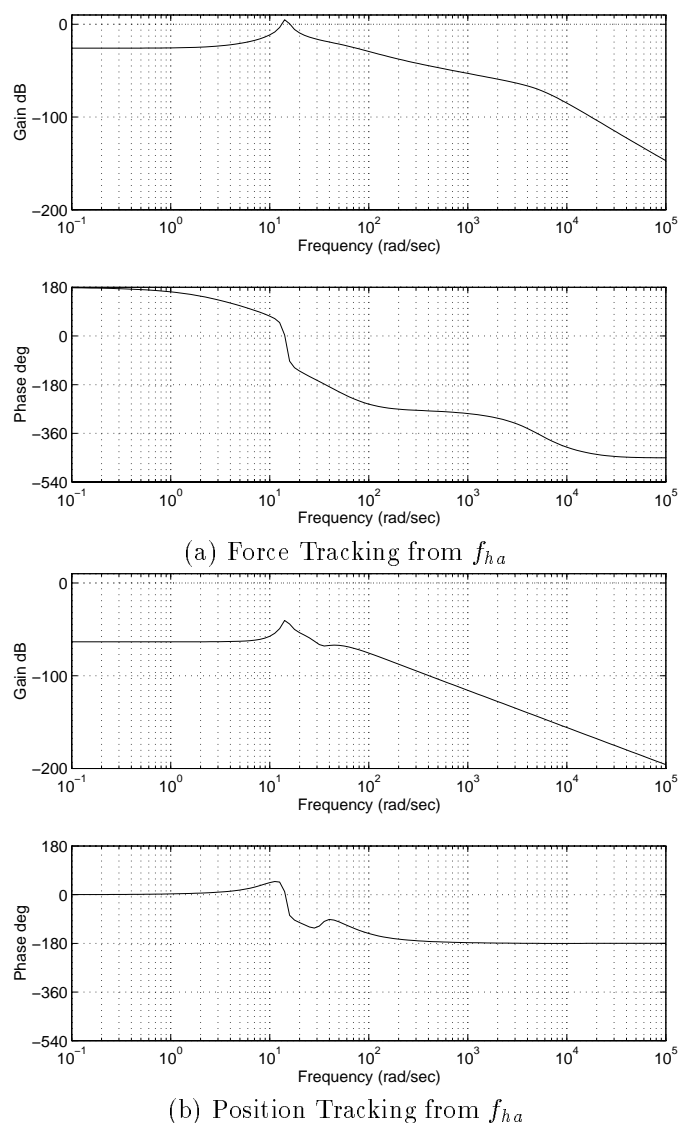
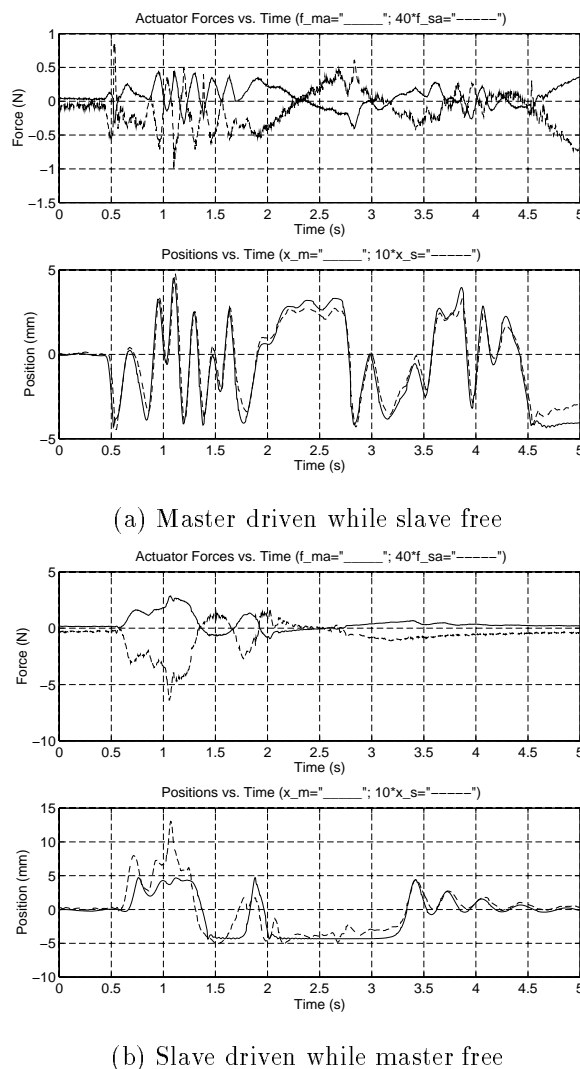


Fig. 12. Experiment for  $\kappa_3$ : Free Motion Tracking

tion in the controller needs careful examination. Higher order controllers are more general and allow greater complexity. However, these come at the expense of more computational time, effectively limiting the system's operating bandwidth. Other control strategies will also be attempted and compared for performance; in particular, strategies based on  $\mu$ -synthesis, adaptive control, sliding mode control, or impedance estimators should provide interesting comparisons.

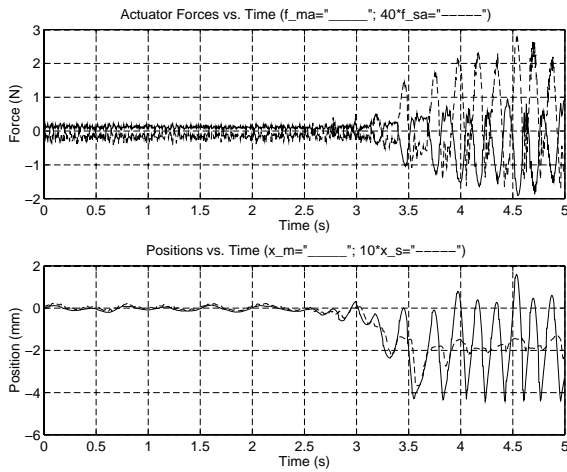
#### REFERENCES

- [1] J. Hill, "Study to design and develop remote manipulator systems," tech. rep., NASA, AMES Research Center (# NAS2-8652, SRI Project 4055), Moffett Field, CA, 1976.
- [2] J. Vertut and P. Coiffet, *Robot Technology, Vol. 3A: Teleoperations and Robotics: Evolution and Development*. Prentice-Hall Series on Robot Technology, Prentice-Hall, 1986.
- [3] I.W. Hunter, S. Lafontaine, P.M.F. Nielsen, P.J. Hunter, and J.M. Hollerbach, "A microrobot for manipulation and dynamical testing of single living cells," in *Proc. IEEE Micro Electro Mechanical Systems*, (Salt Lake City), pp. 102–106, February 1989.
- [4] R.L. Hollis, S.E. Salcudean, and D.W. Abraham, "Towards a tele-nanorobotic manipulation system with atomic scale force feedback and motion resolution," in *Proc. 3rd IEEE Micro Elec-*

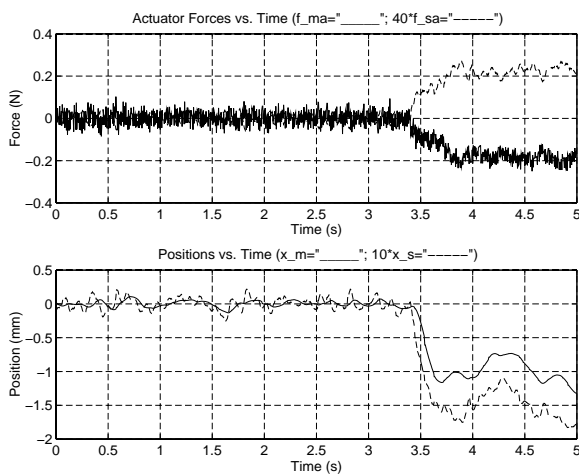
Fig. 13. Tracking Responses for Controller  $\kappa_4$ Fig. 14. Experiment for  $\kappa_4$ : Free Motion Tracking

- tro Mechanical Systems, (Napa Valley, CA), February 1990. 6 pages.
- [5] H. Kazerooni, "Human-robot interaction via the transfer of power and information signals; part i: Dynamics and control analysis," in *Proc. IEEE Robotics and Automation*, (Scottsdale, Arizona), pp. 1632–1640, May 14-18, 1989.
- [6] S.E. Salcudean and J. Yan, "Towards a force-reflecting motion-scaling system for microsurgery," in *Proc. IEEE Conf. Robotics Automat.*, (San Diego, California), pp. 2296–2301, May 9-12 1994.
- [7] J. Yan, "Design and control of a bilateral motion system using magnetic levitation," Master's thesis, University of British Columbia, March 1994.
- [8] R. Hollis, "Magnetically levitated fine motion robot wrist with programmable compliance," October 1989. U.S. Patent number 4,874,998.
- [9] R.L. Hollis, S.E. Salcudean, and P.A. Allan, "A Six Degree-of-Freedom Magnetically Levitated Variable Compliance Fine Motion Wrist: Design, Modelling and Control," *IEEE Transactions on Robotics and Automation*, vol. 7, pp. 320–332, June 1991.
- [10] R.J. Anderson and M.W. Spong, "Bilateral control of operators with time delay," *IEEE Trans. Automat. Cont.*, vol. AC-34, pp. 494–501, May 1989.
- [11] J.-J. E. Slotine and G. Niemeyer, "Transient shaping in force-reflecting teleoperation," in *Fifth Int. Conf. on Advanced Robotics (91 ICAR)*, vol. 1, pp. 261 – 266, 1991.

- [12] G.M.H. Leung, B.A. Francis, and J. Apkarian, "Bilateral controller for teleoperators with time delay via  $\mu$ -synthesis," January 1995.
- [13] G.J. Raju, G.C. Verghese, and T.B. Sheridan, "Design issues in 2-port network models of bilateral remote manipulation," in *Proceedings of the 1989 International Conference on Robotics and Automation*, pp. 1316–1321, 1989.
- [14] Y. Yokokohji and T. Yoshikawa, "Bilateral Control of Master-Slave Manipulators for Ideal Kinesthetic Coupling," in *Proceedings of the IEEE International Conference on Robotics and Automation*, (Nice, France), pp. 849–858, May 10-15 1992.
- [15] D. A. Lawrence, "Designing Teleoperator Architecture for Transparency," in *Proceedings of the IEEE International Conference on Robotics and Automation*, (Nice, France), pp. 1406–1411, May 10-15 1992.
- [16] M. Vidyasagar, *Nonlinear Systems Analysis, 2nd Edition*. Englewood Cliffs, NJ: Prentice-Hall, 1993.
- [17] J.E. Colgate and N. Hogan, "Robust control of dynamically interacting systems," *International Journal of Control*, vol. 48, no. 1, pp. 65–88, 1988.
- [18] J.E. Colgate, "Robust Impedance Shaping Telemanipulation," *IEEE Transactions on Robotics and Automation*, vol. 9, pp. 374–384, August 1993.
- [19] Y. Yokokohji, N. Hosotani, and T. Yoshikawa, "Analysis of Maneuverability and Stability of Micro-Teleoperation Systems," in *Proceedings of the IEEE International Conference on Robotics and Automation*, (San Diego, California), pp. 237–243, May 8-13 1994.



(a)  $\kappa_1$  designed for free motion



(b)  $\kappa_5$  designed for constrained motion

Fig. 15. Experiments in Hard Contact

[20] N. Hogan, "Impedance control: An approach to manipulation, parts i-iii," *ASME J. of Dynamic Systems, Measurement, and Control*, vol. 107, pp. 1-23, March 1985.

[21] B. Hannaford, "A Design Framework for Teleoperators with Kinesthetic Feedback," *IEEE Transactions on Robotics and Automation*, vol. RA-5, pp. 426-434, August 1989.

[22] C.A. Lawn and B. Hannaford, "Performance testing of passive communications and control in teleoperation with time delay," in *Proceedings of the IEEE International Conference on Robotics and Automation*, pp. 776-783, 1993.

[23] S.E. Salcudean, N.M. Wong, and R.L. Hollis, "A Force-Reflecting Teleoperation System with Magnetically Levitated Master and Wrist," in *Proceedings of the IEEE International Conference on Robotics and Automation*, (Nice, France), pp. 1420-1426, May 10-15, 1992.

[24] H. Kazerooni, T.-I. Tsay, and K. Hollerbach, "A Controller Design Framework for Telerobotic Systems," *IEEE Transactions on Control Systems Technology*, vol. 1, pp. 50-62, March 1993.

[25] T. Brooks, "Telerobotic Response Requirements," tech. rep., STX/ROB/90-03, STX Robotics, 4400 Forbes Blvd., Lanham, MD 20706, March 1990.

[26] H. Kazerooni, "Contact instability of the direct drive robot when constrained by a rigid environment," *IEEE Transactions on Automatic Control*, vol. 35, June 1990.

[27] G. Zames, "Feedback and optimal sensitivity; model reference transformations, multiplicative seminorms, and approximate inverses," *IEEE Trans. Automat. Contr.*, vol. AC-26, pp. 301-320, 1981.

[28] J.C. Doyle, K. Glover, P.P. Khargonekar, and B.A. Francis, "State-space solutions to standard  $H^2$  and  $H^\infty$  control problems," *IEEE Trans. Automat. Contr.*, vol. AC-34, pp. 831-846, August 1989.

[29] B.A. Francis, J.W. Helton, and G.Zames, " $H^\infty$ -Optimal Feedback Controllers for Linear Multivariable Systems," *IEEE Trans. Automat. Contr.*, vol. AC-29, pp. 888-900, 1984.

[30] B.A. Francis, *A Course in  $H^\infty$  Control Theory*. Berlin, Heidelberg, New York: Springer-Verlag, 1987.

[31] R.Y. Chiang and M.G. Safonov, *Robust Control Toolbox for use with Matlab*. The MathWorks, Inc., 1992.

[32] J. M. Maciejowski, *Multivariable Feedback Design*. Addison-Wesley, 1989.

[33] J.C. Doyle and G. Stein, "Multivariable feedback design: Concepts for a classical/modern synthesis," *IEEE Trans. on Automat. Contr.*, vol. AC-26, pp. 4-16, February 1981.